marine drugs

MDPI

Article

Salmon-Derived Polydeoxyribonucleotide: A Potent Marine Bioactive Agent Against Skin Photoaging

Byunghan Jeong [1,2], Saekwang Ku [3] and Taeho Oh [1,*]

[1] Department of Veterinary Medicine, Kyungpook National University, 80 Daehak-ro, Buk-gu, Daegu 41566, Republic of Korea; jungbh1@gmail.com
[2] Real Veterinary Dermatology Hospital, 243 Bansong-ro, Dongnae-gu, Busan 47754, Republic of Korea
[3] Department of Anatomy and Histology, College of Korean Medicine, Daegu Haany University, Gyeongsan 38610, Republic of Korea
* Correspondence: thoh@knu.ac.kr

Abstract

The effects of topical salmon-derived polydeoxyribonucleotide (PDRN) against UVB-induced skin photoaging remain incompletely characterized. We investigated the protective effects of 0.25%, 0.5%, and 1% topical PDRN treatment against UVB-induced photoaging in SKH-1 hairless mice, comparing them with 1% L-ascorbic acid (L-AA). Mice were exposed to 0.18 J/cm^2 of UVB three times weekly for 15 weeks, with daily topical treatments. Chronic UVB exposure induced severe wrinkles and edema and reduced cutaneous procollagen type I C-peptide levels. However, PDRN treatments significantly and dose-dependently mitigated these changes. Notably, 0.5% PDRN reduced mean wrinkle length and depth by 41.04% and 44.54%, respectively, with responses of similar magnitude to those observed with 1% L-AA. PDRN treatment increased skin hydration and cutaneous procollagen type I C-peptide and hyaluronan levels, accompanied by increased COL1A1/2 and Has1/2/3 mRNA expression. Furthermore, PDRN restored glutathione levels, reduced thiobarbituric acid-reactive substances (TBARS) levels and superoxide anion production, decreased MPO activity and IL-1β levels, and increased IL-10 levels. These changes were accompanied by decreased p38 MAPK, AKT, and Nox2 mRNA expression and increased TGF-β1 mRNA expression. These preclinical findings support further investigation of topical PDRN, including delivery, safety, and efficacy studies.

Keywords: polydeoxyribonucleotide; photoaging; UVB irradiation; SKH-1 mice; oxidative stress; extracellular matrix

Check for updates

Academic Editor: Lijun You

Received: 15 October 2026
Revised: 29 October 2026
Accepted: 3 November 2026
Published: 4 November 2026

Copyright: © 2026 by the authors. Licensee MDPI, Basel, Switzerland. This article is an open access article distributed under the terms and conditions of the Creative Commons Attribution (CC BY) license.

1. Introduction

Skin serves as a primary barrier against environmental threats, as it regulates both water balance and immune defense [1]. Chronic exposure to ultraviolet B (UVB) radiation is the primary extrinsic factor driving "photoaging," a process characterized by coarse wrinkles formation, dryness, epidermal thickening, and connective tissue degradation [2,3]. Unlike intrinsic aging, photoaging involves a severe remodeling of the extracellular matrix (ECM), including collagen depletion and abnormal elastin accumulation, which occur primarily within the photoexposed dermis [1,4].

The pathogenesis of UVB-induced photoaging is complex, involving reactive oxygen species (ROS) generation, inflammation, keratinocyte apoptosis, and matrix metalloproteinase (MMP)-mediated collagen breakdown [5,6]. Consequently, therapeutic strategies

that mitigate oxidative stress, suppress inflammation, and preserve ECM integrity are essential for preventing premature skin aging [7,8]. For example, the well-established antioxidant L-ascorbic acid (L-AA; vitamin C), known to limit UV-induced inflammation and support collagen biosynthesis, often serves as a positive control in dermatological studies [9,10].

Polydeoxyribonucleotide (PDRN), a potent marine-derived bioactive polymer extracted from salmonid sperm, has emerged as a promising candidate for skin health restoration due to its unique regenerative properties [11].

It exerts anti-inflammatory, angiogenic, and tissue-reparative effects, primarily through the activation of adenosine A2A receptors [12]. While PDRN is well-recognized for its wound-healing capabilities [13], its potential as a functional ingredient in topical therapies specifically targeting UVB-induced skin photoaging and its underlying molecular mechanisms has not been fully assessed.

Although PDRN has demonstrated tissue-reparative and anti-inflammatory properties, the concentration-dependent effects of topical PDRN on UVB-induced skin photoaging have not been adequately characterized. The aim of this study was to evaluate whether topical PDRN mitigates UVB-induced skin photoaging in SKH-1 hairless mice and to characterize associated changes in oxidative stress, inflammatory responses, and extracellular matrix-related endpoints. We hypothesized that PDRN treatment would reduce UVB-induced wrinkle formation and skin edema while improving skin hydration and extracellular matrix-related measurements. To address these objectives, we examined three PDRN concentrations (0.25%, 0.5%, and 1%) alongside a 1% L-ascorbic acid reference group, and assessed morphological, biochemical, histological, immunohistochemical, and gene-expression outcomes.

2. Results

2.1. Effects of PDRN on Wrinkle Formation and Skin Edema

The overall experimental design and timeline are summarized in Figure 1. Chronic UVB exposure resulted in severe photoaging characterized by deep wrinkles and skin edema (Figure 2). Relative to the intact control, mean wrinkle length and depth were greater in the UVB control group (adjusted $p < 0.01$). Topical PDRN-treated groups showed lower wrinkle measures and skin weights than the UVB control group. In the 0.5% PDRN group, mean wrinkle length and depth were 41.04% and 44.54% lower, respectively, than in the UVB control group; the corresponding results for 1% L-AA were of similar magnitude. Group means, SDs, and adjusted comparison p-values are presented in Figure 2 and Supplementary Table S1.

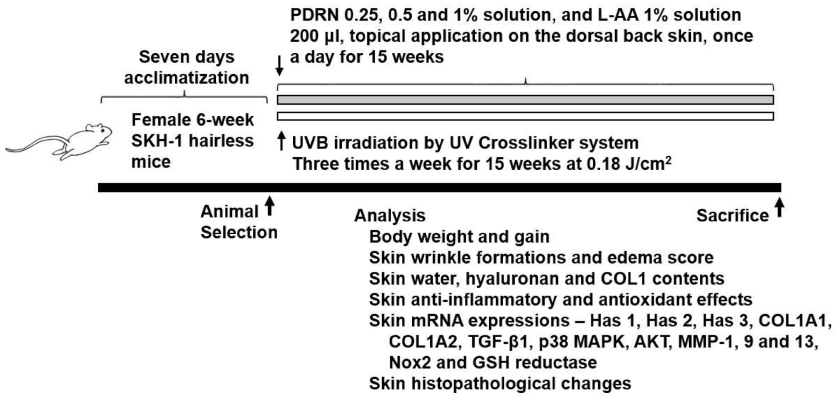


Figure 1. Experimental design and timeline. SKH-1 hairless mice were acclimated for 7 days and then divided into six groups. UVB irradiation (0.18 J/cm^2) was performed three times weekly for 15 weeks, during which topical treatments (Vehicle, L-AA, or PDRN) were applied daily.

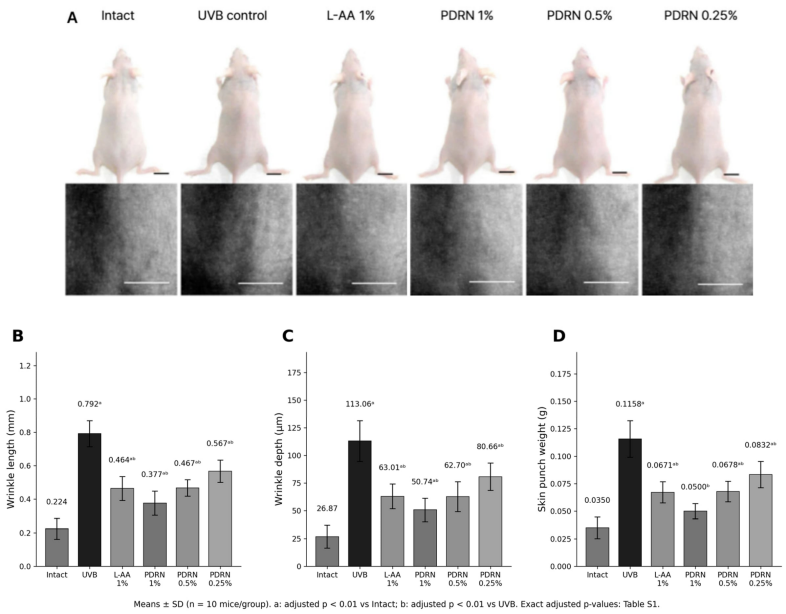


Figure 2. Macroscopic and quantitative analysis of skin wrinkles and edema. (**A**) Representative photographs of dorsal skin and skin replicas (scale bars = 10 mm); (**B**) mean wrinkle length (mm); (**C**) mean wrinkle depth (µm); and (**D**) skin punch weight (g), used as an index of edema. Bars represent mean ± SD ($n = 10$ mice per group), and numerical means are indicated above the bars. Superscript annotations denote a: adjusted $p < 0.01$ versus intact control and b: adjusted $p < 0.01$ versus UVB control, where applicable. All UVB-control versus active-treatment comparisons in panels B–D had adjusted $p < 0.0001$; complete means ± SD and adjusted p-values (to four decimal places or <0.0001), including comparisons with the intact control, are provided in Supplementary Table S1.

2.2. Effects on Skin Hydration, Inflammation, and Oxidative Stress Markers

UVB exposure was associated with lower skin water content and reduced collagen-related and hyaluronan measurements relative to the intact control (adjusted $p < 0.01$; Table 1). PDRN treatment was associated with improvements in these parameters compared with UVB control. Outcomes in the 0.5% PDRN group were of similar magnitude to those recorded for the 1% L-AA group; formal equivalence was not assessed.

Table 1. Effects of topical PDRN applications on skin hydration and extracellular matrix components in skin tissue.

Treatment Groups	Skin Water Contents (%/6 mm Diameter Skin Sections)	Skin COL1 Contents (%, Relative to Intact)	Skin Hyaluronan Contents (ng/mL)
Controls			
Intact	37.21 ± 4.23	113.34 ± 25.73	3.27 ± 0.67
UVB	11.54 ± 1.86 [a]	14.79 ± 6.09 [a]	0.69 ± 0.20 [a]
Reference (L-AA)			
1%	21.72 ± 2.26 [ab]	48.05 ± 12.58 [ab]	1.69 ± 0.41 [ab]
Test materials (PDRN)			
1%	27.23 ± 4.43 [ab]	61.47 ± 13.08 [ab]	2.14 ± 0.35 [ab]
0.5%	21.90 ± 2.79 [ab]	49.62 ± 11.90 [ab]	1.68 ± 0.29 [ab]
0.25%	18.15 ± 1.55 [ab]	36.24 ± 10.45 [ab]	1.33 ± 0.28 [ab]

Values are expressed as the means ± SD of 10 hairless mice. UVB = Ultraviolet B; L-AA = L-ascorbic acid; PDRN = polydeoxyribonucleotide; COL1 = collagen, type I. Significant differences are represented using superscript letters: [a] indicates $p < 0.01$ for comparisons with the intact control and, [b] indicates $p < 0.01$ for comparisons with the UVB control. Statistical significance was determined using one-way ANOVAs followed by Tukey's HSD or Dunnett's T3 post hoc tests, depending on homogeneity of variance results.

To evaluate the anti-inflammatory and antioxidant effects of PDRN, we measured cutaneous inflammatory cytokines and oxidative stress markers (Table 2). UVB irradiation

elevated myeloperoxidase (MPO) activity and IL-1β levels while decreasing IL-10 levels relative to the intact control. UVB exposure was also associated with lower glutathione (GSH), higher thiobarbituric acid-reactive substances (TBARS, reported as malondialdehyde equivalents), and higher superoxide anion production. Topical PDRN was associated with lower inflammatory and oxidative stress-related measurements relative to UVB controls, with a graded pattern across the tested concentrations. The 0.5% PDRN and 1% L-AA groups showed responses of similar magnitude for several outcomes; equivalence was not formally tested.

Table 2. Effects of topical PDRN applications on inflammatory cytokines and oxidative stress markers in skin tissues.

Treatment Groups	Myeloperoxidase (Number of Neutrophils × 10^5/mg Protein)	Interleukin-1β (pg/100 mg of Protein)	Interleukin-10 (pg/100 mg of Protein)	Glutathione (μM/mg of Protein)	Lipid Peroxidation (TBARS; Reported as nM MDA Equivalents/mg Protein)	Superoxide Anion Production (NBT Reduction as OD_{600})
Controls						
Intact	1.50 ± 0.41	22.72 ± 10.44	343.30 ± 54.16	2.62 ± 1.10	0.39 ± 0.14	0.31 ± 0.11
UVB	16.11 ± 3.67 [a]	91.24 ± 18.17 [a]	115.00 ± 25.36 [a]	0.26 ± 0.13 [a]	2.07 ± 0.50 [a]	1.42 ± 0.30 [a]
Reference (L-AA)						
1%	6.76 ± 1.31 [ab]	48.61 ± 10.23 [ab]	184.70 ± 14.35 [ab]	0.76 ± 0.18 [ab]	1.17 ± 0.20 [ab]	0.63 ± 0.13 [ab]
Test materials (PDRN)						
1%	4.66 ± 1.42 [ab]	39.96 ± 11.55 [b]	227.50 ± 44.14 [ab]	0.91 ± 0.13 [ab]	0.73 ± 0.15 [ab]	0.48 ± 0.12 [b]
0.5%	6.78 ± 1.79 [ab]	48.50 ± 12.76 [ab]	185.80 ± 14.21 [ab]	0.75 ± 0.12 [ab]	1.15 ± 0.19 [ab]	0.62 ± 0.13 [ab]
0.25%	8.79 ± 1.69 [ab]	63.06 ± 11.21 [ab]	160.10 ± 11.56 [ab]	0.64 ± 0.10 [ab]	1.41 ± 0.10 [ac]	0.87 ± 0.12 [ab]

Values are expressed as the mean ± SD of 10 hairless mice. UVB = Ultraviolet B; L-AA = L-ascorbic acid; PDRN = polydeoxyribonucleotide; NBT = nitroblue tetrazolium; OD_{600} = optical density at 600 nm. Significant differences are represented using superscript letters: [a] indicates $p < 0.01$ for comparisons with the intact control, [b] indicates $p < 0.01$ for comparisons with the UVB control, and [c] indicates $p < 0.05$ for comparisons with the UVB control. Statistical significance was determined using one-way ANOVAs followed by Tukey's HSD or Dunnett's T3 post hoc tests, depending on homogeneity of variance results.

2.3. Effects on mRNA Expression of Photoaging-Related Genes

We examined the effects of PDRN on photoaging-related gene expression using qPCR (Table 3). Compared with the intact control, the UVB control group showed significantly increased mRNA expression of MMP-1, MMP-9, MMP-13, Nox2, p38 MAPK, and AKT and significantly decreased expression of TGF-β1 and glutathione reductase. In contrast, Has1, Has2, Has3, COL1A1, and COL1A2 mRNA expression did not differ significantly between the intact and UVB control groups. Compared with the UVB control, PDRN treatment significantly decreased the expression of MMPs, Nox2, p38 MAPK, and AKT and increased the expression of TGF-β1, glutathione reductase, Has1–3, COL1A1, and COL1A2. These findings indicate that PDRN treatment was associated with changes in the expression of genes related to extracellular matrix remodeling and oxidative stress.

Table 3. Changes in skin mRNA expression levels in UVB-exposed hairless mice.

	Controls		Reference (L-AA)	Test Materials (PDRN)		
	Intact	UVB	1%	1%	0.5%	0.25%
TGF-β1	1.13 ± 0.19	0.17 ± 0.06 [a]	0.41 ± 0.08 [ab]	0.58 ± 0.14 [ab]	0.41 ± 0.11 [ab]	0.31 ± 0.04 [ab]
p38 MAPK	1.06 ± 0.14	5.77 ± 1.14 [a]	3.17 ± 0.61 [ab]	2.21 ± 0.58 [ab]	3.18 ± 0.78 [ab]	3.74 ± 0.49 [ab]
AKT	1.08 ± 0.17	3.40 ± 0.76 [a]	1.91 ± 0.23 [ab]	1.51 ± 0.22 [ab]	1.93 ± 0.23 [ab]	2.07 ± 0.26 [ab]
Has1	1.06 ± 0.15	1.01 ± 0.33	2.38 ± 0.37 [ab]	3.27 ± 0.79 [ab]	2.37 ± 0.39 [ab]	1.83 ± 0.16 [ab]
Has2	1.11 ± 0.18	1.07 ± 0.25	2.54 ± 0.92 [ab]	3.49 ± 0.65 [ab]	2.53 ± 0.66 [ab]	1.94 ± 0.46 [ab]
Has3	1.08 ± 0.18	1.04 ± 0.17	2.44 ± 0.61 [ab]	3.36 ± 1.04 [ab]	2.47 ± 0.53 [ab]	1.87 ± 0.31 [ab]
COL1A1	1.14 ± 0.19	1.17 ± 0.22	2.65 ± 0.71 [ab]	3.63 ± 0.84 [ab]	2.64 ± 0.63 [ab]	2.00 ± 0.29 [ab]

Table 3. *Cont.*

	Controls		Reference (L-AA)	Test Materials (PDRN)		
	Intact	**UVB**	**1%**	**1%**	**0.5%**	**0.25%**
COL1A2	1.17 ± 0.21	1.24 ± 0.46	2.85 ± 0.67 ^{ab}	3.77 ± 0.69 ^{ab}	2.83 ± 0.69 ^{ab}	2.13 ± 0.10 ^{ab}
MMP-1	1.12 ± 0.19	6.65 ± 1.18 ^{a}	3.56 ± 0.36 ^{ab}	1.98 ± 0.36 ^{ab}	3.53 ± 0.77 ^{ab}	4.60 ± 0.62 ^{ab}
MMP-9	1.14 ± 0.20	4.41 ± 0.61 ^{a}	2.34 ± 0.51 ^{ab}	1.76 ± 0.33 ^{ab}	2.39 ± 0.48 ^{ab}	3.01 ± 0.31 ^{ab}
MMP-13	1.10 ± 0.14	5.38 ± 0.54 ^{a}	2.91 ± 0.64 ^{ab}	2.23 ± 0.41 ^{ab}	2.90 ± 0.69 ^{ab}	3.81 ± 0.56 ^{ab}
GSH reductase	1.07 ± 0.16	0.20 ± 0.06 ^{a}	0.56 ± 0.11 ^{ab}	0.63 ± 0.21 ^{ab}	0.56 ± 0.13 ^{ab}	0.42 ± 0.10 ^{ab}
Nox2	1.11 ± 0.31	4.74 ± 0.80 ^{a}	2.72 ± 0.50 ^{ab}	1.87 ± 0.22 ^{ab}	2.73 ± 0.33 ^{ab}	3.17 ± 0.31 ^{ab}

Values are expressed as the mean ± SD of the relative expression/β-actin mRNA in 10 hairless mice. UVB = ultraviolet B; L-AA = L-ascorbic acid; PDRN = polydeoxyribonucleotide; TGF = transforming growth factor; MAPK = mitogen-activated protein kinase; AKT = protein kinase B; COL1 = collagen, type I; COL1A1 = COL1, alpha 1; COL1A2 = COL1, alpha 2; GSH = glutathione; Has = hyaluronic acid synthase; Nox2 = the gp91phox subunit of the phagocyte NADPH oxidase. Significant differences are represented using superscript letters: ^{a} indicates $p < 0.01$ for comparisons with the intact control and ^{b} indicates $p < 0.01$ for comparisons with the UVB control. Statistical significance was determined using one-way ANOVAs followed by Tukey's HSD or Dunnett's T3 post hoc tests, depending on homogeneity of variance results.

2.4. Histological and Immunohistochemical Analysis

Histopathological examination using hematoxylin and eosin (H&E) and Masson's trichrome staining revealed that UVB exposure caused marked epidermal thickening, inflammatory cell infiltration, and an increased collagen-stained area in the dermis (Figure 3). PDRN treatment attenuated these UVB-induced histological changes.

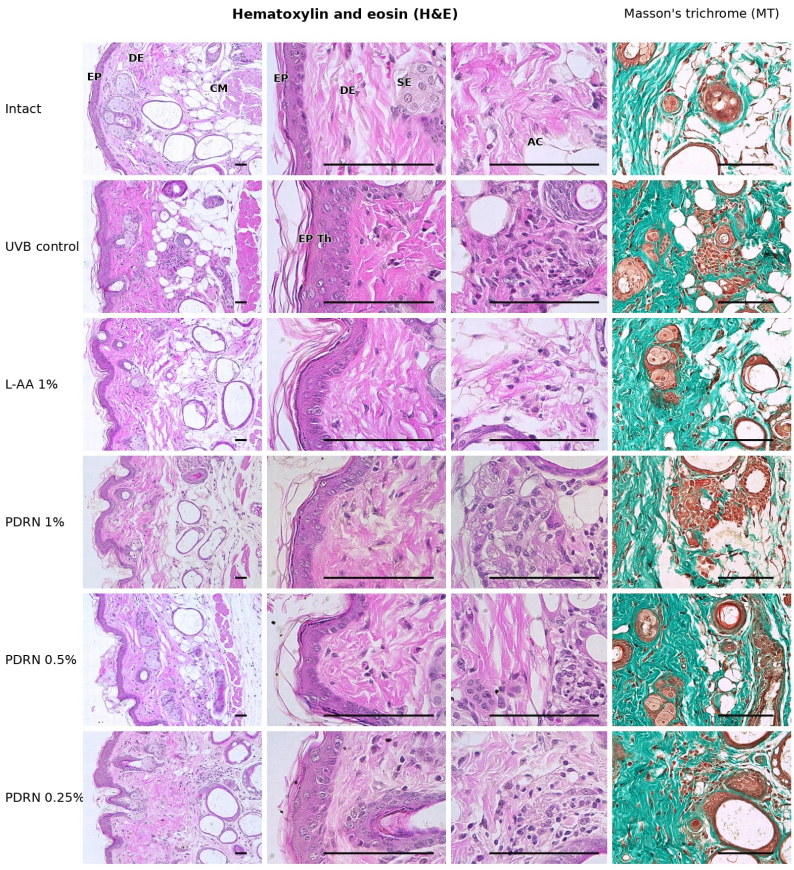


Figure 3. Representative images showing the histological staining of dorsal skin tissues (scale bars = 200 μm). Sections were stained with hematoxylin and eosin (left three panels) or Masson's trichrome (MT) (right panel).

Immunohistochemical analyses confirmed the cytoprotective effects of PDRN (Figure 4). The UVB control group showed increased proportions of epidermal cells positive for NT, 4-HNE, cleaved caspase-3, and cleaved PARP, together with an increased MMP-9-immunopositive area in the dermis. Topical PDRN treatment significantly reduced the proportions of these immunopositive epidermal cells and the dermal MMP-9-immunopositive area. Quantitative immunohistochemical results are summarized in Table 4.

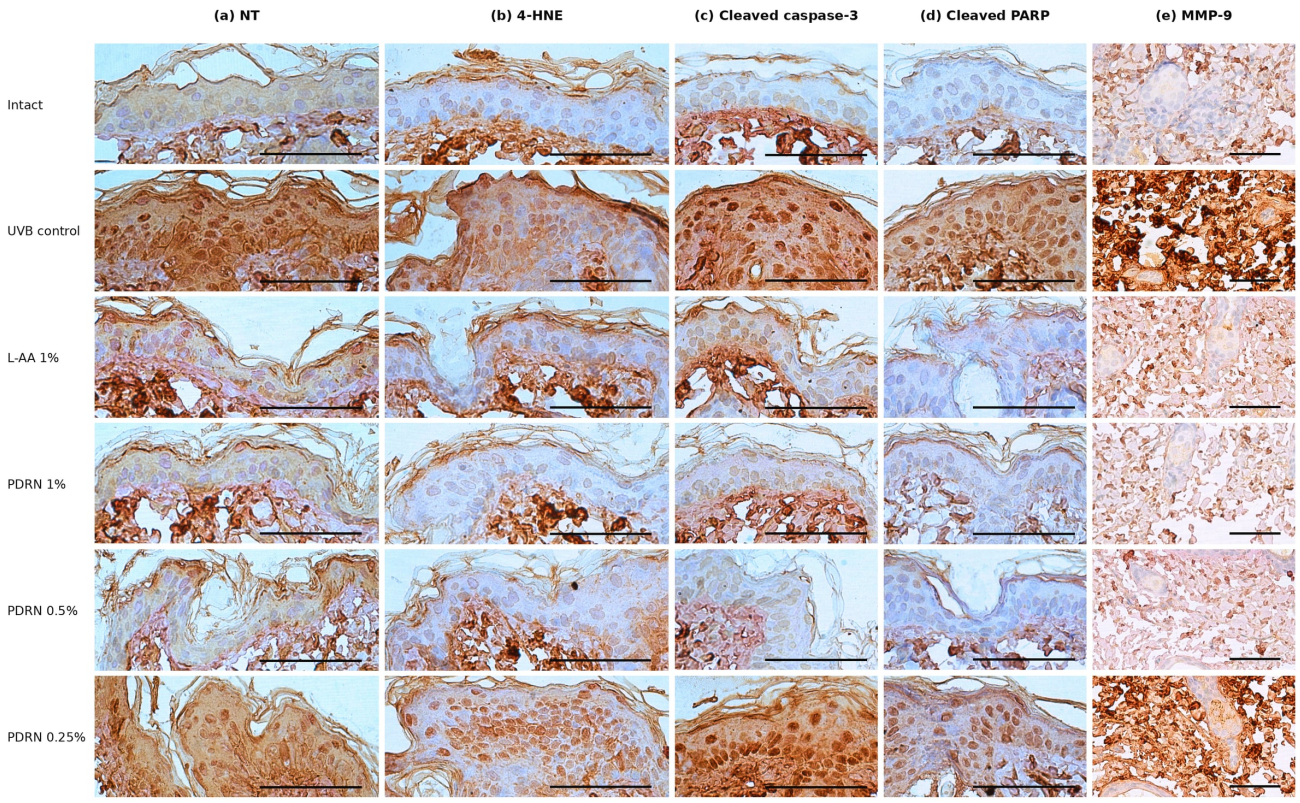


Figure 4. Representative images showing the immunohistochemical staining of oxidative stress and apoptosis markers, including (**a**) nitrotyrosine (NT), (**b**) 4-hydroxynonenal (4-HNE), (**c**) cleaved caspase-3, (**d**) cleaved PARP, and (**e**) MMP-9 (scale bars = 150 µm).

Table 4. Quantitative immunohistochemical analysis of dorsal skin.

	Controls		Reference (L-AA)	Test Material (PDRN)		
	Intact	**UVB**	**1%**	**1%**	**0.5%**	**0.25%**
Epidermis (cells/100 epithelial cells)						
Nitrotyrosine	10.20 ± 4.57	84.00 ± 10.58 [a]	46.00 ± 10.50 [ab]	34.80 ± 11.78 [ab]	46.20 ± 14.00 [ab]	62.60 ± 10.96 [ab]
4-HNE	10.60 ± 3.89	80.80 ± 8.18 [a]	46.20 ± 11.56 [ab]	31.60 ± 13.33 [ab]	45.40 ± 10.92 [ab]	56.80 ± 10.80 [ab]
Cleaved caspase-3	17.80 ± 3.19	85.20 ± 8.01 [a]	44.60 ± 10.50 [ab]	33.80 ± 10.97 [ab]	44.80 ± 11.20 [ab]	60.00 ± 11.27 [ab]
Cleaved PARP	15.20 ± 3.91	77.00 ± 12.55 [a]	39.40 ± 11.28 [ab]	30.20 ± 11.17 [b]	40.40 ± 10.99 [ab]	54.20 ± 10.97 [ab]
Dermis (%/mm^2)						
MMP-9	19.63 ± 5.53	74.03 ± 11.12 [a]	38.25 ± 11.04 [ab]	30.60 ± 11.58 [b]	36.85 ± 14.72 [b]	52.93 ± 10.35 [ab]

Values are expressed as the mean ± SD of 10 hairless mice. UVB = ultraviolet B; L-AA = L-ascorbic acid; PDRN = polydeoxyribonucleotide; 4-HNE = 4-hydroxynonenal; PARP = poly(ADP-ribose) polymerase; MMP = matrix metalloprotease. Significant differences are represented using superscript letters: [a] indicates $p < 0.01$ for comparisons with the intact control, [b] indicates $p < 0.01$ for comparisons with the UVB control. Statistical significance was determined using one-way ANOVAs followed by Tukey's HSD or Dunnett's T3 post hoc tests, depending on homogeneity of variance results.

3. Discussion

Ultraviolet B radiation is a major environmental factor contributing to extrinsic skin aging, or photoaging, which is characterized by wrinkle formation, dehydration, and connective tissue degradation [1–3]. In this study, we investigated the protective effects of salmon-derived PDRN on UVB-induced photoaging in hairless mice. Our findings demonstrate that topical PDRN application attenuates UVB-induced oxidative stress, inflammation, and alterations in extracellular matrix-related parameters, accompanied by changes in p38 MAPK, AKT, and TGF-β1 mRNA expression. Notably, 0.5% PDRN produced improvements of similar magnitude to those observed with 1% L-AA across several measured endpoints, supporting the potential of this marine-derived material as a topical ingredient for skin photoprotection.

A naturally occurring polymer, PDRN is typically obtained from the sperm of salmon trout or related species. It has drawn attention for its unique pharmacological properties, including anti-inflammatory activities and an ability to enhance angiogenesis [11,12]. While previous studies have focused on wound healing [13], our results demonstrate that it plays a role in protecting against UVB-induced damage, which is consistent with recent studies on other marine-derived substances [14,15].

Oxidative stress triggered by UVB irradiation depletes endogenous antioxidants and promotes the production of ROS, leading to DNA damage and inflammation [4]. In our study, UVB exposure significantly reduced cutaneous GSH levels and increased lipid peroxidation (TBARS levels) and superoxide anion production. However, PDRN treatments restored GSH levels and suppressed oxidative markers in a dose-dependent manner. This aligns with previous findings that antioxidants derived from natural sources possess substantial photoprotective potential [8].

Inflammation is another critical driver of photoaging. UVB exposure induces cutaneous inflammatory responses that contribute to photoaging [5]. We showed that PDRN treatment significantly decreased MPO activity and IL-1β levels while increasing levels of the anti-inflammatory cytokine IL-10. This anti-inflammatory effect likely contributed to the reductions in skin edema and epidermal hyperplasia observed in the histological analyses [12,16].

The structural integrity of the skin relies on the balance between collagen synthesis and degradation. UV-induced ROS activate MAPK signaling and increase MMP expression, while impaired TGF-β/Smad signaling contributes to reduced collagen synthesis [6,17]. In the current study, UVB irradiation increased the mRNA expression of p38 MAPK, AKT, MMP-1, MMP-9, and MMP-13. PDRN treatment reduced these UVB-induced increases and increased TGF-β1, COL1A1, and COL1A2 mRNA expression compared with the UVB control. These findings suggest that changes in extracellular matrix remodeling may contribute to the reduced wrinkle depth and length observed in PDRN-treated mice [18].

Skin hydration is essential for maintaining skin elasticity and barrier function. Hyaluronic acid, synthesized by hyaluronic acid synthases, plays a key role in retaining skin moisture [19]. We found that PDRN treatment increased Has1, Has2, and Has3 mRNA expression and cutaneous hyaluronan levels compared with the UVB control. This suggests that PDRN not only protects collagen but also enhances the skin's moisturizing capacity, which is crucial for preventing the dryness associated with photoaging [14].

The 0.5% PDRN group showed responses of similar magnitude to the 1% L-AA group for several measured outcomes. However, these descriptive similarities do not establish statistical equivalence or non-inferiority, and the present study was not designed to determine an optimal topical concentration. Concentration selection for subsequent formulation studies should take into account the full dose–response profile, topical delivery, local tolerability, and formulation stability.

Taken together, the observed improvements in wrinkle measures, hydration, inflammatory markers, and extracellular matrix-related endpoints support further investigation of salmon-derived PDRN as a candidate topical ingredient for photoaging-related applications. Translation to human dermatology or cosmeceutical use remains preliminary because the present evidence derives from a UVB-exposed mouse model. Skin penetration and local bioavailability of topically applied PDRN were not directly established, and long-term local safety and clinical efficacy in humans were not investigated. Future studies should optimize formulation and concentration, directly evaluate skin delivery and tolerability, and confirm efficacy in appropriately controlled translational and human studies. Changes in mRNA expression should be interpreted as associations rather than direct evidence of pathway activation or inhibition.

4. Materials and Methods

4.1. Chemicals and Reagents

The test material, referred to as polydeoxyribonucleotide (PDRN) in this study, was purchased from Sigma-Aldrich (St. Louis, MO, USA) under the product name "deoxyribonucleic acid sodium salt from salmon testes" (catalog no. D1626; CAS no. 438545-06-3; lot no. 102840926). All other chemicals and reagents were of analytical grade. Primary antibodies against cleaved caspase-3 (catalog no. 9661; dilution, 1:400), cleaved PARP (catalog no. sc-23461-R; 1:100), and nitrotyrosine (catalog no. 06-284; 1:200) were obtained from Cell Signaling Technology (Danvers, MA, USA), Santa Cruz Biotechnology (Santa Cruz, CA, USA), and Millipore (Billerica, MA, USA), respectively. Antibodies against 4-hydroxynonenal (catalog no. ab46545; 1:100) and MMP-9 (catalog no. ab38898; 1:100) were obtained from Abcam (Cambridge, UK). Secondary antibodies were obtained from Vector Laboratories Inc. (Burlingame, CA, USA; included in Vectastain Elite ABC Kit).

4.2. Animals and Ethics Statement

Six-week-old female SKH-1 hairless mice were purchased from OrientBio (Seongnam, Korea). The mice were housed in a controlled environment at 20–25 °C and 50–55% relative humidity under a 12 h light–dark cycle, with free access to standard rodent chow and water. All experimental procedures complied with national guidelines for the care and use of laboratory animals and were approved by the Institutional Animal Care and Use Committee of Daegu Haany University (Gyeongsan, Republic of Korea; approval no. DHU2025-023; approval date: 12 May 2025).

4.3. Experimental Design, UVB Irradiation, and Topical Treatment Application

After a 7-day acclimatization period, 60 mice were randomly allocated to six groups (n = 10 independent animals per group):

Intact Control: No UVB, vehicle treatment
UVB Control: UVB irradiation + vehicle treatment
L-AA 1%: UVB irradiation + 1% L-AA (positive control)
PDRN 0.25%: UVB irradiation + 0.25% PDRN
PDRN 0.5%: UVB irradiation + 0.5% PDRN
PDRN 1%: UVB irradiation + 1% PDRN

UVB irradiation was performed using a CL-3000M UV crosslinker (Analytik Jena, Upland, CA, USA; peak wavelength, 312 nm) at 0.18 J/cm^2 per exposure, three times per week for 15 weeks. The intact controls were not exposed to UVB. Test materials were prepared in a 0.5% carboxymethyl cellulose (CMC) vehicle, and PDRN solutions were sonicated for 1 h during preparation. Treatments (200 µL/mouse) were applied to the dorsal skin once daily, 1 h following irradiation on UVB-exposure days and at the corresponding

time on non-irradiation days. The topical application method and UVB schedule were based on the laboratory study protocol (OTH017-UVB).

The initial formulation plan considered PDRN concentrations as high as 5%; however, the 5% preparation was excessively viscous and difficult to apply topically. Accordingly, 1% was selected as the highest practicable PDRN concentration, and lower concentrations of 0.25% and 0.5% were included to examine concentration-related responses. The L-ascorbic acid (L-AA) positive-comparator concentration was likewise set at 1% to match the highest tested PDRN concentration. This matching was a study-design choice and does not imply that the two substances are equipotent.

4.4. Skin Wrinkle, Edema, and Hydration Assessment

At the end of the treatment period, dorsal skin replicas were obtained with a Repliflo Cartridge Kit (CuDerm Corp., Dallas, TX, USA) under 2–3% isoflurane anesthesia. Replicas were placed horizontally and illuminated with a fixed-intensity light source at an angle of approximately 40° to generate wrinkle shadows; monochrome images were captured and analyzed using a Skin-Visiometer SV600 (Courage & Khazaka, Cologne, Germany) to determine average wrinkle length and depth. Dorsal skin was sampled after the final treatment, and the weight of a standardized 6 mm-diameter skin punch was measured as an index of skin edema. Skin water content was determined using a moisture analyzer (MB23; Ohaus, Pine Brook, NJ, USA) on 6 mm skin specimens and expressed as a percentage. These measurements followed the established laboratory UVB photoaging assessment workflow.

4.5. Biochemical Analyses

To assess extracellular-matrix-related outcomes, dorsal skin specimens were homogenized in radioimmunoprecipitation assay (RIPA) buffer using mechanical disruption and ultrasound, and supernatants were collected after refrigerated centrifugation. Procollagen type I C-peptide was determined with a commercial kit (MK101; Takara Bio, Tokyo, Japan), with absorbance measured at 450 nm. For hyaluronan determination, skin samples were defatted with acetone, dried and weighed, heated in 50 mM Tris/HCl buffer (pH 7.8), and proteolytically digested in 1% actinase E at 40 °C for one week. Following deproteinization with 10% trichloroacetic acid and neutralization, hyaluronan was measured with a mouse ELISA kit (MBS161603; MyBioSource, San Diego, CA, USA) at 450 nm. The IL-1β (ab100705; Abcam) and IL-10 (ab108870; Abcam) contents of skin homogenates were measured using commercial ELISA kits according to the manufacturers' instructions. Myeloperoxidase (MPO) activity was quantified in skin homogenates using a kinetic colorimetric assay with o-dianisidine and hydrogen peroxide in phosphate buffer (pH 6.0), with absorbance measured at 450 nm; the output was normalized to protein content.

Reduced glutathione (GSH) was assessed in skin homogenates prepared in 100 mM phosphate buffer (pH 8.0) containing 5 mM EDTA. After trichloroacetic acid precipitation and centrifugation, o-phthalaldehyde was added and fluorescence measured after 15 min (excitation 350 nm, emission 420 nm); a GSH calibration series (0–75 µM) was used and results were normalized to protein content.

Lipid peroxidation was quantified by the thiobarbituric acid-reactive substances (TBARS) procedure, not a chemically selective MDA assay. Homogenates were deproteinized with 10% trichloroacetic acid, treated with 0.67% thiobarbituric acid and incubated at 100 °C for 15 min. Absorbance at 535 and 572 nm was used to estimate TBARS expressed as malondialdehyde (MDA) equivalents per mg protein. Superoxide-related NBT reduction was assessed by incubating skin homogenates with nitroblue tetrazolium (1 mg/mL) at 37 °C for 1 h, solubilizing the resulting formazan in KOH/DMSO and reading absorbance

at 600 nm. Each biochemical endpoint was measured once per mouse-derived sample, without technical duplicate or triplicate measurements.

4.6. Quantitative PCR

Total RNA was extracted from dorsal skin samples using TRIzol (Invitrogen, Carlsbad, CA, USA), and contaminating DNA was removed with DNase I (DNA-free kit, AM1906; Thermo Fisher Scientific, Rockford, IL, USA). Reverse transcription was conducted using the High-Capacity cDNA Reverse Transcription Kit (Thermo Fisher Scientific). Quantitative real-time PCR was performed on a CFX96 Real-Time System (Bio-Rad, Hercules, CA, USA) using SYBR Green chemistry. The laboratory protocol specifies an initial 50 °C step for 2 min and 95 °C for 10 min, followed by 95 °C for 15 s and 60 °C for 1 min, with subsequent melting-curve assessment. Primer sequences are shown in Table 5. Relative mRNA expression of TGF-β1, p38 MAPK, AKT, Has1–3, COL1A1/2, MMP-1/9/13, Nox2 and glutathione reductase was analyzed using the 2^(−ΔΔCt) approach with β-actin as the reference gene. For statistical analysis, the biological replicate was the individual mouse ($n = 10$ per treatment group); one final expression value per animal was entered into the dataset. Each qPCR target was measured in a single technical reaction per mouse-derived sample; no technical replicate reactions were performed.

Table 5. Sequences of the oligonucleotide primers used for quantitative reverse transcription polymerase chain reaction RT-qPCR.

Target Gene	5′–3′	Sequence	GenBank Accession Number
Has1	Forward Reverse	GCTACTTCCACTGTGTGTCCTG CTAAGCATTCGGTTGGTGAGGTG	NM_008215
Has2	Forward Reverse	CATCTGTGGAGATGGTGAAGGTC AGCCATCCAGTATCTCACGCTG	NM_008216
Has3	Forward Reverse	CCTTGGCAACTCAGTGGACTAC TGGACATCTCCTCCAACACCTC	NM_008217
COL1A1	Forward Reverse	CCTCAGGGTATTGCTGGACAAC CAGAAGGACCTTGTTTGCCAGG	NM_007742
COL1A2	Sense Antisense	TTCTGTGGGTCCTGCTGGGAAA TTGTCACCTCGGATGCCTTGAG	NM_007743
TGF-β1	Sense Antisense	TGATACGCCTGAGTGGCTGTCT CACAAGAGCAGTGAGCGCTGAA	NM_011577
p38 MAPK	Sense Antisense	CCGAACGATACCAGAACCTGTC ACGCAACTCTCGGTAGGTCCTT	NM_011951
AKT	Sense Antisense	GGACTACTTGCACTCCGAGAAG CATAGTGGCACCGTCCTTGATC	NM_009652
MMP-1	Sense Antisense	AGGAAGGCGATATTGTGCTCTCC TGGCTGGAAAGTGTGAGCAAGC	NM_032006
MMP-9	Sense Antisense	GCTGACTACGATAAGGACGGCA TAGTGGTGCAGGCAGAGTAGGA	NM_013599
MMP-13	Sense Antisense	GATGACCTGTCTGAGGAAGACC GCATTTCTCGGAGCCTGTCAAC	NM_008607
GSH reductase	Sense Antisense	GTTTACCGCTCCACACATCCTG GCTGAAAGAAGCCATCACTGGTG	NM_010344

Table 5. *Cont.*

Target Gene	5′–3′	Sequence	GenBank Accession Number
Nox2	Sense Antisense	TGGCGATCTCAGCAAAAGGTGG GTACTGTCCCACCTCCATCTTG	NM_007807
β-actin	Sense Antisense	CATTGCTGACAGGATGCAGAAGG TGCTGGAAGGTGGACAGTGAGG	NM_007393

Has = hyaluronic acid synthase; COL1 = collagen, type I; COL1A1 = COL1, alpha 1; COL1A2 = COL1, alpha 2; TGF = transforming growth factor; MAPK = mitogen-activated protein kinase; AKT = protein kinase B; MMP = matrix metalloprotease; GSH = glutathione; Nox2 = gp91phox subunit of the phagocyte NADPH oxidase. All qPCR primer pairs were obtained from OriGene Technologies (Rockville, MD, USA).

4.7. Histopathology and Immunohistochemistry

Dorsal skin specimens were fixed in 10% neutral-buffered formalin, processed into paraffin blocks and sectioned at 3–4 μm. Hematoxylin and eosin staining was used for epidermal thickness and dermal inflammatory-cell assessment, and Masson's trichrome staining for evaluation of dermal collagen-stained regions. Imaging and histomorphometric quantification were performed using a light microscope equipped with a digital camera and iSolution FL version 9.1 (IMT i-Solution Inc., Burnaby, BC, Canada). The laboratory protocol specified analysis of a central field where possible, with at least one histological field from each animal; the histopathologist was blinded to group allocation. For immunohistochemistry, sections underwent heat-based antigen retrieval in 10 mM citrate buffer (pH 6.0), endogenous peroxidase blocking with 0.3% hydrogen peroxide for 30 min, and nonspecific-binding blockade with normal horse serum for 1 h. Sections were incubated overnight at 4 °C with antibodies to nitrotyrosine (NT), 4-hydroxynonenal (4-HNE), cleaved caspase-3, cleaved PARP or MMP-9; an appropriate biotinylated secondary antibody and avidin–biotin-peroxidase detection system were applied, followed by color development. Immunopositive epidermal cells were expressed per 100 epithelial cells, and dermal MMP-9-immunopositive area was quantified as a percentage of dermal area. Each mouse was treated as an independent biological unit for the group-level summaries.

4.8. Statistical Analysis

Data are presented as means ± standard deviations (SDs), with the individual mouse as the biological experimental unit ($n = 10$ per group). Statistical analyses were conducted using SPSS software version 18.0 (SPSS Inc., Chicago, IL, USA). Data were analyzed by one-way analysis of variance (ANOVA) across six groups. Levene's test was used to assess the homogeneity of variances for each outcome; Tukey's honestly significant difference (HSD) post hoc test was applied when equal variances were supported, and Dunnett's T3 procedure when they were not. Adjusted pairwise comparisons with the intact and UVB controls are reported in Tables 1–4 and Supplementary Table S1. Statistical significance was evaluated at $p < 0.05$; the letter annotations in each table specify the exact threshold and comparator. Corrected summary values and annotations were independently checked against the archived mouse-level SPSS datasets. Each assay result was based on one technical determination per animal-derived sample; the reported $n = 10$ reflects biological replicates rather than repeated measurements of a single sample.

5. Conclusions

Topical PDRN treatment in UVB-exposed SKH-1 hairless mice was associated with reduced wrinkle formation and edema as well as improvements in cutaneous hydration, extracellular-matrix-related measurements, and inflammatory and oxidative stress markers.

Relative to the UVB control, 0.5% PDRN reduced mean wrinkle length by 41.04% (0.792 to 0.467 mm) and wrinkle depth by 44.54% (113.06 to 62.70 μm). The corresponding mean skin punch weight declined from 0.1158 to 0.0678 g (41.45%). In the same comparison, skin hyaluronan increased from 0.69 to 1.68 ng/mL and glutathione (GSH) from 0.26 to 0.75 μM/mg protein, whereas IL-1β decreased from 91.24 to 48.50 pg/100 mg protein. Several measurements in the 0.5% PDRN group were of similar magnitude to those in the 1% L-AA reference group, although equivalence was not formally tested. These findings support additional dose- and formulation-optimization studies, together with evaluation of topical penetration, safety and clinical efficacy before potential translation to human skin applications.

Supplementary Materials: The following supporting information can be downloaded at: https://www.mdpi.com/article/10.3390/md24110395/s1, Table S1: Descriptive statistics and adjusted pairwise comparisons of wrinkle length, wrinkle depth, and skin punch weight.

Author Contributions: Conceptualization, B.J. and T.O.; methodology, B.J. and S.K.; software, B.J.; validation, B.J., S.K. and T.O.; formal analysis, B.J.; investigation, B.J. and S.K.; resources, S.K. and T.O.; data curation, B.J.; writing—original draft preparation, B.J.; writing—review and editing, S.K. and T.O.; visualization, B.J.; supervision, T.O. and S.K.; project administration, T.O.; funding acquisition, T.O. All authors have read and agreed to the published version of the manuscript.

Funding: This research received no external funding.

Institutional Review Board Statement: The animal study protocol was approved by the Institutional Animal Care and Use Committee of Daegu Haany University (Approval No. DHU2025-023; Date: 12 May 2025).

Data Availability Statement: The raw data supporting the conclusions of this article will be made available by the authors on request.

Acknowledgments: We would like to thank the members of the Department of Veterinary Medicine at Kyungpook National University for their technical support.

Conflicts of Interest: The authors declare no conflicts of interest.

References

1. Gu, Y.; Han, J.; Jiang, C.; Zhang, Y. Biomarkers, oxidative stress and autophagy in skin aging. *Ageing Res. Rev.* **2020**, *59*, 101036. [CrossRef] [PubMed]
2. Rittié, L.; Fisher, G.J. Natural and sun-induced aging of human skin. *Cold Spring Harb. Perspect. Med.* **2015**, *5*, a015370. [CrossRef] [PubMed]
3. Parrado, C.; Mercado-Saenz, S.; Perez-Davo, A.; Gilaberte, Y.; Gonzalez, S.; Juarranz, A. Environmental stressors on skin aging. Mechanistic insights. *Front. Pharmacol.* **2019**, *10*, 759. [CrossRef]
4. Chen, J.; Liu, Y.; Zhao, Z.; Qiu, J. Oxidative stress in the skin: Impact and related protection. *Int. J. Cosmet. Sci.* **2021**, *43*, 495–509. [CrossRef] [PubMed]
5. Salminen, A.; Kaarniranta, K.; Kauppinen, A. Photoaging: UV radiation-induced inflammation and immunosuppression accelerate the aging process in the skin. *Inflamm. Res.* **2022**, *71*, 817–831. [CrossRef] [PubMed]
6. Pittayapruek, P.; Meephansan, J.; Prapapan, O.; Komine, M.; Ohtsuki, M. Role of matrix metalloproteinases in photoaging and photocarcinogenesis. *Int. J. Mol. Sci.* **2016**, *17*, 868. [CrossRef] [PubMed]
7. Shin, J.W.; Kwon, S.H.; Choi, J.Y.; Na, J.I.; Huh, C.H.; Choi, H.R.; Park, K.C. Molecular mechanisms of dermal aging and anti-aging approaches. *Int. J. Mol. Sci.* **2019**, *20*, 2126. [CrossRef] [PubMed]
8. Dunaway, S.; Odin, R.; Zhou, L.; Ji, L.; Zhang, Y.; Kadekaro, A.L. Natural antioxidants: Multiple mechanisms to protect skin from solar radiation. *Front. Pharmacol.* **2018**, *9*, 392. [CrossRef] [PubMed]
9. Boo, Y.C. Ascorbic acid (Vitamin C) as a cosmeceutical to increase dermal collagen for skin anti-aging purposes: Emerging combination therapies. *Antioxidants* **2022**, *11*, 1663. [CrossRef]
10. Pullar, J.M.; Carr, A.C.; Vissers, M.C.M. The roles of vitamin C in skin health. *Nutrients* **2017**, *9*, 866. [CrossRef] [PubMed]

11. Galeano, M.; Pallio, G.; Irrera, N.; Mannino, F.; Bitto, A.; Altavilla, D.; Vaccaro, M.; Squadrito, G.; Arcoraci, V.; Colonna, M.R.; et al. Polydeoxyribonucleotide: A promising biological platform to accelerate impaired skin wound healing. *Pharmaceuticals* **2021**, *14*, 1103. [CrossRef] [PubMed]
12. Squadrito, F.; Bitto, A.; Irrera, N.; Pizzino, G.; Pallio, G.; Minutoli, L.; Altavilla, D. Pharmacological activity and clinical use of PDRN. *Front. Pharmacol.* **2017**, *8*, 224. [CrossRef] [PubMed]
13. Squadrito, F.; Bitto, A.; Altavilla, D.; Arcoraci, V.; De Caridi, G.; De Feo, M.E.; Corrao, S.; Pallio, G.; Sterrantino, C.; Minutoli, L.; et al. The effect of PDRN, an adenosine receptor A2A agonist, on the healing of chronic diabetic foot ulcers: Results of a clinical trial. *J. Clin. Endocrinol. Metab.* **2014**, *99*, E746–E753. [PubMed]
14. Kim, J.; Lee, N.; Chun, Y.S.; Lee, S.H.; Ku, S.K. Krill oil's protective benefits against ultraviolet B-induced skin photoaging in hairless mice and in vitro experiments. *Mar. Drugs* **2023**, *21*, 479. [CrossRef] [PubMed]
15. Fonseca, S.; Amaral, M.N.; Reis, C.P.; Custódio, L. Marine natural products as innovative cosmetic ingredients. *Mar. Drugs* **2023**, *21*, 170. [CrossRef] [PubMed]
16. Subedi, L.; Lee, T.H.; Wahedi, H.M.; Baek, S.H.; Kim, S.Y. Resveratrol-enriched rice attenuates UVB-ROS-induced skin aging via downregulation of inflammatory cascades. *Oxid. Med. Cell. Longev.* **2017**, *2017*, 8379539. [CrossRef] [PubMed]
17. Quan, T.; He, T.; Kang, S.; Voorhees, J.J.; Fisher, G.J. Solar ultraviolet irradiation reduces collagen in photoaged human skin by blocking transforming growth factor-β type II receptor/Smad signaling. *Am. J. Pathol.* **2004**, *165*, 741–751. [CrossRef] [PubMed]
18. Sun, Z.; Park, S.Y.; Hwang, E.; Zhang, M.; Seo, S.A.; Lin, P.; Yi, T.H. Thymus vulgaris alleviates UVB irradiation induced skin damage via inhibition of MAPK/AP-1 and activation of Nrf2-ARE antioxidant system. *J. Cell. Mol. Med.* **2017**, *21*, 336–348. [CrossRef] [PubMed]
19. Papakonstantinou, E.; Roth, M.; Karakiulakis, G. Hyaluronic acid: A key molecule in skin aging. *Derm.-Endocrinol.* **2012**, *4*, 253–258. [CrossRef] [PubMed]

Disclaimer/Publisher's Note: The statements, opinions and data contained in all publications are solely those of the individual author(s) and contributor(s) and not of MDPI and/or the editor(s). MDPI and/or the editor(s) disclaim responsibility for any injury to people or property resulting from any ideas, methods, instructions or products referred to in the content.